Topological Quantum Computation-From Basic Concepts to First Experiments

Article *in* Science · March 2013

DOI: 10.1126/science.1231473 · Source: PubMed

2 authors, including:

Ady Stern
Weizmann Institute of Science
246 PUBLICATIONS **17,015** CITATIONS

SEE PROFILE

The breadth of research in solid-state quantum information science is largely what makes the field so exciting. Advances achieved in one system are often directly applicable to many others, and solving the challenges that arise leads to breakthroughs that carry over to other fields of science and engineering. Clearly, the synergies between solid state and atomic physics are accelerating discoveries and demonstrations in both fields. Besides the potential we already recognize for quantum machines, our quest for greater control over quantum systems will surely lead to new materials and applications we have yet to imagine, just as the pioneers of classical computing could not have predicted exactly how the digital revolution has shaped our information age.

References and Notes

1. T. D. Ladd *et al.*, *Nature* **464**, 45 (2010).
2. R. Hanson, D. D. Awschalom, *Nature* **453**, 1043 (2008).
3. G. E. Moore, *Electronics* **38**, 114 (1965).
4. D. Loss, D. P. DiVincenzo, *Phys. Rev. A* **57**, 120 (1998).
5. R. Hanson, L. P. Kouwenhoven, J. R. Petta, S. Tarucha, L. M. K. Vandersypen, *Rev. Mod. Phys.* **79**, 1217 (2007).
6. J. R. Petta, H. Lu, A. C. Gossard, *Science* **327**, 669 (2010).
7. S. Nadj-Perge, S. M. Frolov, E. P. A. M. Bakkers, L. P. Kouwenhoven, *Nature* **468**, 1084 (2010).
8. J. Berezovsky, M. H. Mikkelsen, N. G. Stoltz, L. A. Coldren, D. D. Awschalom, *Science* **320**, 349 (2008).
9. D. Press, T. D. Ladd, B. Zhang, Y. Yamamoto, *Nature* **456**, 218 (2008).
10. W. B. Gao, P. Fallahi, E. Togan, J. Miguel-Sanchez, A. Imamoglu, *Nature* **491**, 426 (2012).
11. K. De Greve *et al.*, *Nature* **491**, 421 (2012).
12. G. de Lange, Z. H. Wang, D. Ristè, V. V. Dobrovitski, R. Hanson, *Science* **330**, 60 (2010).
13. C. A. Ryan, J. S. Hodges, D. G. Cory, *Phys. Rev. Lett.* **105**, 200402 (2010).
14. H. Bluhm *et al.*, *Nat. Phys.* **7**, 109 (2011).
15. A. M. Tyryshkin *et al.*, *Nat. Mater.* **11**, 143 (2011).
16. M. Steger *et al.*, *Science* **336**, 1280 (2012).
17. B. E. Kane, *Nature* **393**, 133 (1998).
18. J. J. L. Morton, D. R. McCamey, M. A. Eriksson, S. A. Lyon, *Nature* **479**, 345 (2011).
19. J. J. Pla *et al.*, *Nature* **489**, 541 (2012).
20. A. Morello *et al.*, *Nature* **467**, 687 (2010).
21. J. R. Petta *et al.*, *Science* **309**, 2180 (2005).
22. J. J. Pla *et al.*, http://arxiv.org/abs/1302.0047.
23. B. M. Maune *et al.*, *Nature* **481**, 344 (2012).
24. F. Jelezko, T. Gaebel, I. Popa, A. Gruber, J. Wrachtrup, *Phys. Rev. Lett.* **92**, 076401 (2004).
25. G. Balasubramanian *et al.*, *Nat. Mater.* **8**, 383 (2009).
26. G. D. Fuchs, V. V. Dobrovitski, D. M. Toyli, F. J. Heremans, D. D. Awschalom, *Science* **326**, 1520 (2009).
27. L. Childress *et al.*, *Science* **314**, 281 (2006).
28. M. V. G. Dutt *et al.*, *Science* **316**, 1312 (2007).
29. P. Neumann *et al.*, *Science* **329**, 542 (2010).
30. W. Pfaff *et al.*, *Nat. Phys.* **9**, 29 (2013).
31. P. C. Maurer *et al.*, *Science* **336**, 1283 (2012).
32. L. Robledo *et al.*, *Nature* **477**, 574 (2011).
33. B. B. Buckley, G. D. Fuchs, L. C. Bassett, D. D. Awschalom, *Science* **330**, 1212 (2010).
34. E. Togan *et al.*, *Nature* **466**, 730 (2010).
35. L. Trifunovic *et al.*, *Phys. Rev. X* **2**, 011006 (2012).
36. R. Raussendorf, J. Harrington, *Phys. Rev. Lett.* **98**, 190504 (2007).
37. M. D. Shulman *et al.*, *Science* **336**, 202 (2012).
38. F. Dolde *et al.*, http://arxiv.org/abs/1212.2804 (2012).
39. P. Rabl *et al.*, *Nat. Phys.* **6**, 602 (2010).
40. S. Bose, *Contemp. Phys.* **48**, 13 (2007).
41. R. P. G. McNeil *et al.*, *Nature* **477**, 439 (2011).
42. S. Hermelin *et al.*, *Nature* **477**, 435 (2011).
43. H. J. Kimble, *Nature* **453**, 1023 (2008).
44. K. J. Vahala, *Nature* **424**, 839 (2003).
45. J. P. Reithmaier *et al.*, *Nature* **432**, 197 (2004).
46. K. Hennessy *et al.*, *Nature* **445**, 896 (2007).
47. I. Fushman *et al.*, *Science* **320**, 769 (2008).
48. S. G. Carter *et al.*, http://arxiv.org/abs/1211.4540 (2012).
49. I. Aharonovich, A. D. Greentree, S. Prawer, *Nat. Photonics* **5**, 397 (2011).
50. H. Bernien *et al.*, http://arxiv.org/abs/1212.6136 (2012).
51. L. C. Bassett, F. J. Heremans, C. G. Yale, B. B. Buckley, D. D. Awschalom, *Phys. Rev. Lett.* **107**, 266403 (2011).
52. A. Wallraff *et al.*, *Nature* **431**, 162 (2004).
53. K. D. Petersson *et al.*, *Nature* **490**, 380 (2012).
54. L. DiCarlo *et al.*, *Nature* **467**, 574 (2010).
55. G. D. Fuchs, G. Burkard, P. V. Klimov, D. D. Awschalom, *Nat. Phys.* **7**, 789 (2011).
56. J. R. Weber *et al.*, *Proc. Natl. Acad. Sci. U.S.A.* **107**, 8513 (2010).
57. W. F. Koehl, B. B. Buckley, F. J. Heremans, G. Calusine, D. D. Awschalom, *Nature* **479**, 84 (2011).
58. R. Kolesov *et al.*, http://arxiv.org/abs/1301.5215 (2013).
59. T. D. Ladd, K. Sanaka, Y. Yamamoto, A. Pawlis, K. Lischka, *Phys. Status Solidi B* **247**, 1543 (2010).
60. G. D. Fuchs *et al.*, *Nat. Phys.* **6**, 668 (2010).
61. D. M. Toyli, C. D. Weis, G. D. Fuchs, T. Schenkel, D. D. Awschalom, *Nano Lett.* **10**, 3168 (2010).

Acknowledgments: D.D.A., L.C.B., and E.L.H. acknowledge support from the Air Force Office of Scientific Research and the Defense Advanced Research Projects Agency (DARPA); A.S.D. from the Australian Research Council (project CE11E0096) and the U.S. Army Research Office (contract W911NF-08-1-0527); and J.R.P. from the Sloan and Packard Foundations, Army Research Office grant W911NF-08-1-0189, NSF grants DMR-0819860 and DMR-0846341, and DARPA QuEST grant HR0011-09-1-0007.

10.1126/science.1231364

REVIEW

Topological Quantum Computation—From Basic Concepts to First Experiments

Ady Stern[1]* and Netanel H. Lindner[2,3]

Quantum computation requires controlled engineering of quantum states to perform tasks that go beyond those possible with classical computers. Topological quantum computation aims to achieve this goal by using non-Abelian quantum phases of matter. Such phases allow for quantum information to be stored and manipulated in a nonlocal manner, which protects it from imperfections in the implemented protocols and from interactions with the environment. Recently, substantial progress in this field has been made on both theoretical and experimental fronts. We review the basic concepts of non-Abelian phases and their topologically protected use in quantum information processing tasks. We discuss different possible realizations of these concepts in experimentally available solid-state systems, including systems hosting Majorana fermions, their recently proposed fractional counterparts, and non-Abelian quantum Hall states.

The principal obstacles on the road to quantum computing are noise and decoherence. By noise, we mean imperfections in the execution of the operations on the qubits (quantum bits). Decoherence arises when the quantum system that encodes the qubits becomes entangled with its environment, which is a bigger, uncontrolled system. There are two approaches to tackling these barriers. One is based on complete isolation of the computer from its environment, careful elimination of noise, and protocols for quantum correction of unavoidable errors. Enormous progress has been achieved in this direction in the past few years. The other approach, which is at the root of topological quantum computation, is very different. It uses a non-Abelian state of matter (*1*–*10*) to encode and manipulate quantum information in a nonlocal manner. This nonlocality endows the information with immunity to the effects of noise and decoherence (*2*–*6*).

Non-Abelian States of Matter

Several properties define a non-Abelian state of matter (*1*, *2*, *6*–*10*). It is a quantum system whose

[1]Department of Condensed Matter Physics, Weizmann Institute of Science, Rehovot 76100, Israel. [2]Institute of Quantum Information and Matter, California Institute of Technology, Pasadena, CA 91125, USA. [3]Department of Physics, California Institute of Technology, Pasadena, CA 91125, USA.

*To whom correspondence should be addressed. E-mail: adiel.stern@weizmann.ac.il

ground state is separated from the excited part of the spectrum by an energy gap. The elementary particles of the system may form collective composite particles, known as "non-Abelian anyons." When that occurs, the ground state becomes degenerate. In the limit of a large number of anyons, N, the ground-state degeneracy is λ^N, and the anyon is said to have a "quantum dimension" of λ. This degeneracy is not a result of any obvious symmetry of the system. As such, it is robust and cannot be lifted with the application of any local perturbation (*11*).

Transformations between the degenerate ground states may be induced by exchanging the anyons' positions. The canonical example is that of a two-dimensional (2D) system, where anyons may be regarded as point particles. Imagine a set of anyons that are initially positioned on a plane at $(R_1 \ldots R_N)$. They are made to move along a set of trajectories $[R_1(t) \ldots R_N(t)]$ that ends with their positions permuted. The motion is slow enough not to excite the system out of the subspace of ground states. When viewed in a 3D plot, the set of trajectories, known also as world lines, $R_i(t)$ look like entangled strands of spaghetti. A "braid" is defined as a set of spaghetti configurations that can be deformed to one another without spaghetti strands being cut. Remarkably, the unitary transformation implemented by the motion of the anyons depends only on the braid and is independent of the details of the trajectories. These unitary transformations must satisfy a set of conditions that result from their topological nature, such as the Yang-Baxter equation (Fig. 1A).

Notably, for the braid in which two anyons of types a and b are encircled by a third that is far away (Fig. 1B), the corresponding transformation will not be able to resolve the two anyons' types; from a distance they would look as if they "fused" to one anyon, of type c. The fusion of a pair of non-Abelian anyons may result in several different outcomes that are degenerate in energy when the anyons are far away from one another (leading to the ground-state degeneracy). The degeneracy is split when the fused anyons get close. The list of cs to which any a-b pair may fuse constitutes the "fusion rules." For each anyon of type a, there is an "anti-anyon" $\bar{a}$ such that the two may annihilate one another, or be created as a pair.

Topological Quantum Computation

The properties of non-Abelian states that are important for our discussion are the quantum dimensions of the anyons, the unitary transformations that they generate by braiding, and their fusion rules. Different non-Abelian systems differ in these properties. To turn a non-Abelian system into a quantum computer, we first create pairs of anyons and anti-anyons from the "vacuum," the state of zero anyons. In the simplest computational model, a qubit is composed of a group of several anyons, and its two states, $|0\rangle$ and $|1\rangle$, are two possible fusion outcomes of these anyons. (A qudit is formed if there are more than two possible fusion outcomes.) The creation from the vacuum initializes qubits in a well-defined state. The unitary gates are implemented by the braid transformations (Fig. 1C). At the end of the computation, the state is read off by measuring the fusion outcome of the anyons (*2*–*6*).

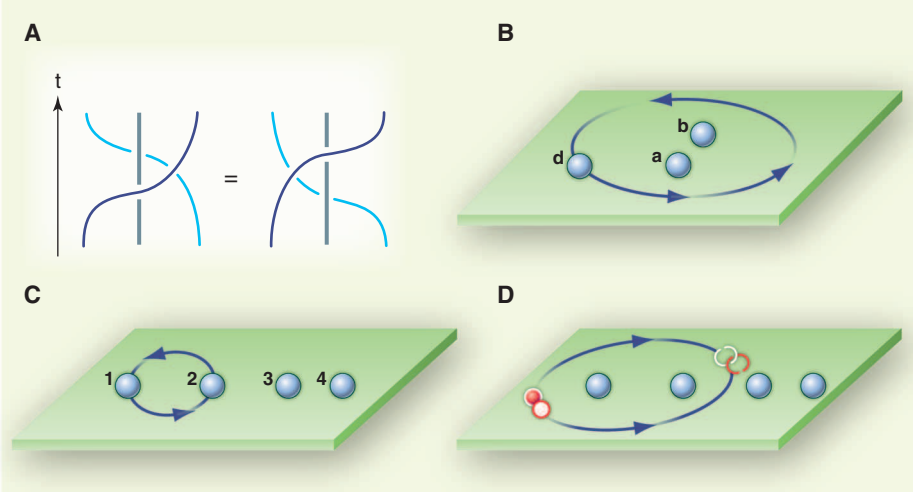

Fig. 1. (**A**) The Yang-Baxter equation states that two exchange paths that can be deformed into each other without cutting the world lines of the particles (blue curves) define the same braid. (**B**) Two anyons labeled a and b are encircled by a third anyon d. The resulting transformation depends only on the fusion outcome of a and b. (**C**) A canonical construction for a qubit, in a system of Ising anyons, consists of four anyons that together fuse to the vacuum. The two possible states can then be labeled by the fusion charge, say, of the left pair. A single qubit $\pi/4$ gate can be used by exchanging anyons 1 and 2 (depicted), whereas a Hadamard gate can be used by exchanging anyons 2 and 3. Such a construction can be realized using Majorana fermions. (**D**) Decoherence of information encoded in the ground-state space. Thermal and quantum fluctuations nucleate a quasiparticle-antiquasiparticle pair (red, white). The pair encircles two anyons encoding quantum information, and annihilates. The result of the process depends on the fusion charge of the two anyons, leading to decoherence of the encoded quantum information.

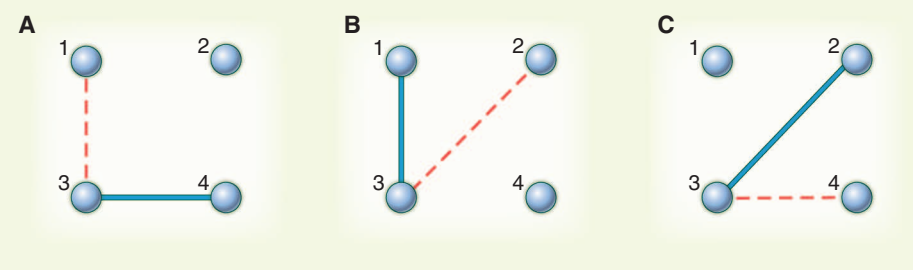

Fig. 2. Braiding in a system hosting Majorana fermions (zero modes or their fractionalized counterparts). For a manipulation of the subspace of ground states to lead to a topological result, the number of ground states should remain fixed. (**A**) Two zero modes initially at locations 1 and 2 are to be interchanged. A pair of coupled zero modes, 3 and 4, is created from the vacuum and may reside, for example, at the two ends of a short wire. As long as 3 and 4 are coupled (blue line), they are not zero modes and do not change the degeneracy of the ground state. Next, location 1 is coupled to 3 and 4 (red dashed line). The coupled system of 1, 3, and 4 must still harbor a zero mode. Thus, this step does not vary the degeneracy of the ground state, but it does redistribute the wave function of that zero mode among the three coupled sites. Location 4 is then decoupled from 1 and 3, and the localized zero mode is now at location 4. The outcome is then that 1 was copied to location 4. (**B**) In a similar fashion, 2 is copied to location 1. (**C**) Finally, 1 is copied from location 4 to location 2. At the end of this series, 3 and 4 are again coupled to one another, but 1 and 2 have been interchanged.

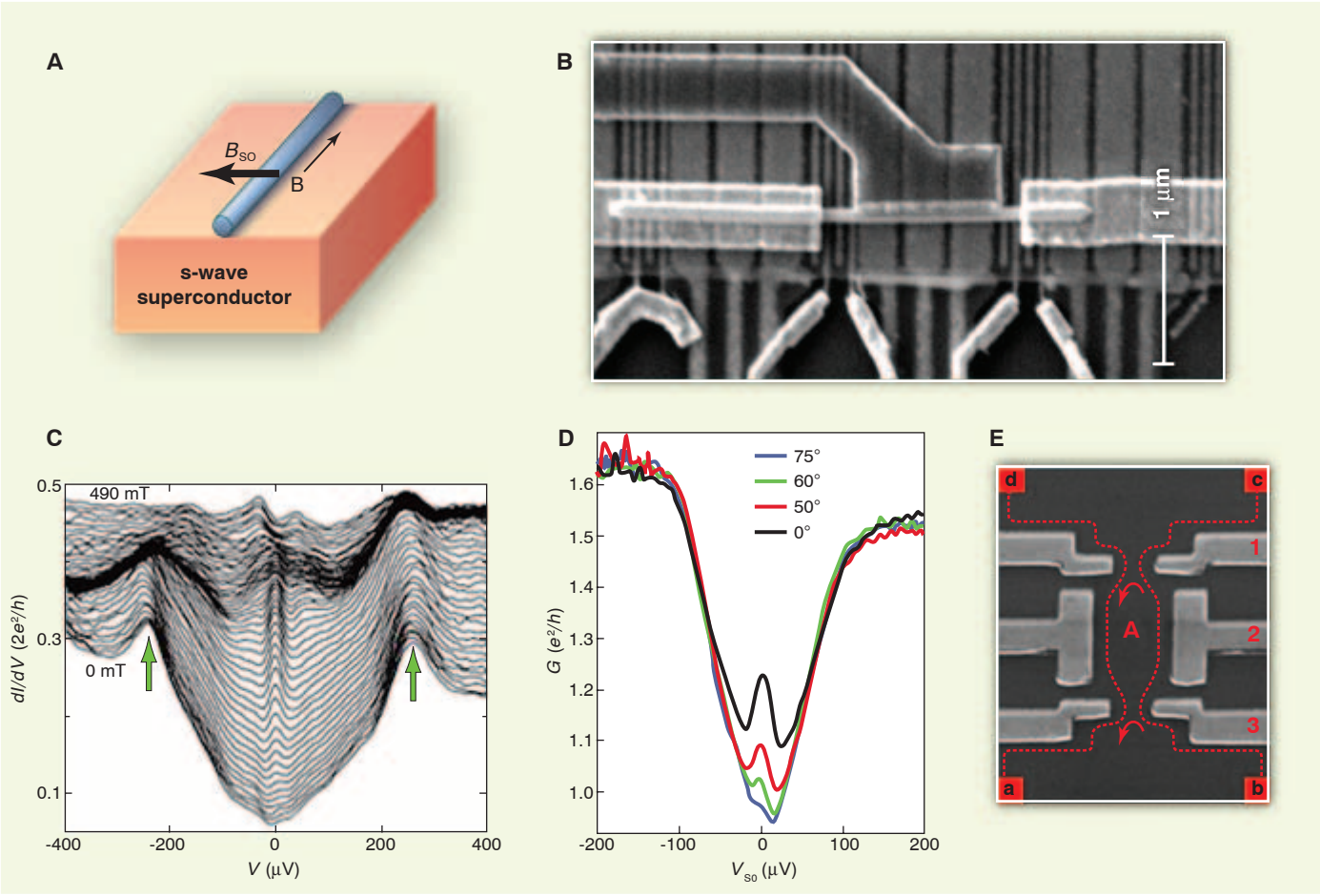

Fig. 3. Majorana end modes in a quantum wire. (**A**) A schematic plot of the sample: a quantum wire lying on a superconductor. B is the magnetic field that couples to the electron's spin, and B_{so} is the effective magnetic field induced by spin-orbit scattering. (**B**) A picture of the sample. Scale bar, 1 μm. (**C** and **D**) The measured differential conductance as a function of voltage at a range of magnetic fields (C) and magnetic field orientation (D) in the experiments reported in (*28*) and (*29*), respectively. The peak at zero voltage may be a sign of a Majorana fermion zero mode. (**E**) The experimental device of the type used in (*50*, *58*) to measure interference of quasiparticles in the ν = 5/2 state. The periodicity of the interference pattern as a function of magnetic field and gate voltage reflects the non-Abelian nature of the quasiparticles (*54*–*56*). Indicated are the interference loop (A), the interfering trajectories (dashed lines), ohmic contacts (a to d), and gates (numbered). [(A), (B), and (C) reprinted from (*28*); (D) reprinted from (*29*) by permission of Macmillan Publishers Ltd., copyright 2012; (E) reprinted from (*58*)]

The process outlined above is immune to noise and decoherence. The only mechanism that may alter the quantum state of the qubit in an uncontrolled fashion is a quantum or thermal fluctuation that creates an anyon–anti-anyon pair from the vacuum; the pair braids around two of the qubit's anyons, and finally annihilates (Fig. 1D). The probability for such a process decreases exponentially with decreasing temperature and with increasing distance between the anyons.

A quantum computer needs to have a minimal set of gates that allow it to efficiently approximate any unitary transformation in its space of logical states. Such a set is commonly called universal (*12*, *13*). For example, a universal set may be composed of two single-qubit gates and a two-qubit controlled-not gate (CNOT). For some non-Abelian states, all of these gates may be carried out in a topologically protected way (*2*, *4*–*6*). Fortunately, even when that is not the case, universality may still be obtained by combining topological and nontopological operations, as shown below (*14*, *15*).

Zero Modes and Majorana Fermions

A useful concept for understanding the stability of the degeneracy of the ground state in non-Abelian systems is that of localized "zero modes" (*16*, *17*). These are operators that act only within the subspace of ground states, and whose operation is confined to a localized spatial region. Generally, the number of independent operators that transfer the system between orthogonal ground states must be even. Thus, when there is only one such operator acting within a given spatial region, it must be Hermitian (note that Hermitian conjugation does not change the location of the operator). Consequently, it must have a partner in a different spatial region. If the system is subjected to a perturbation that acts locally within one of the regions, the local zero mode cannot be eliminated, because its partner is not subjected to that perturbation.

The position and wave function of the zero modes depend on the parameters of the system. Braiding operations are carried out by a cyclic trajectory in this parameter space. The braiding of world lines in two dimensions (*18*, *19*) is a particular example of topologically distinct classes of cyclic trajectories in the parameter space. More generally, the unitary transformation applied by a cycle is determined by the topological class to which the cycle belongs. This allows for braiding operations in systems that are not 2D, such as networks of 1D wires (*20*–*22*) (Fig. 2).

The simplest non-Abelian states of matter, those that carry Majorana fermions (*16*, *17*), can

be explained using the concept of zero modes. Such systems usually combine spin-orbit coupling, superconductivity, and Zeeman coupling to the electron spin (*23*–*27*). In superconductors, operators that take the system from one energy state to another are superpositions of electron creation and annihilation operators. In certain conditions, localized zero modes occur, in which the amplitude for the creation and annihilation operators is equal in magnitude, and the resulting operator is Hermitian. These operators are commonly referred to as Majorana fermions. The non-Abelian state of matter occurs when the zero modes are spatially separated from one another. Like all zero modes, Majorana fermions occur in pairs. A pair of Majorana fermions form a complex conventional fermion that spans a Hilbert space of two dimensions. The quantum dimension of a single Majorana fermion is therefore $\sqrt{2}$.

Because a superconductor is gapped, Majorana fermions in a superconducting system can only occur where the superconducting gap closes locally. In 2D systems, Majorana fermions are to be found in vortex cores (*16*, *18*), whereas in 1D systems they are to be found at the interfaces between different types of superconductivity, or at the system's ends (*17*). In vortex cores of s-wave superconductors, the presence of two spin directions per each electronic state does not allow for an isolated Majorana fermion zero mode. The places to look for isolated Majorana fermions are superconductors with only one spin direction per each electronic state. Examples are superconductors with spin-polarized p-wave pairing (*16*, *17*), surfaces of 3D and edges of 2D topological insulators (*23*, *24*), and 2D/1D systems featuring both spin-orbit and Zeeman couplings (*25*–*27*) in proximity to superconductors.

Recent experiments (*28*–*32*) support the existence of Majorana fermions at the ends of semiconducting wires in which strong spin-orbit coupling, together with Zeeman coupling of the spin to a magnetic field, creates a range of densities at which spin degeneracy is removed. The wires are made superconducting through their proximity to a superconductor, and zero modes are expected to form at their ends, which are separated from metallic contacts by potential barriers. When a current is driven through the wires in the absence of the end modes, the combination of the barriers and the superconducting gap suppresses the current at low voltages. The Majorana end modes allow current to flow, resulting in a sharp peak in the wires' differential conductance at zero voltage. This peak was observed in several experiments (Fig. 3) and its characteristics are consistent with Majorana end modes in quantum wires.

Although these are encouraging observations, it is still too early to identify them unambiguously as originating from Majorana fermions. The wires used in the experiments were short enough that coupling between the two ends may be expected to split the degeneracy between the end modes. Future experiments may observe the decay of this splitting with increasing wire length. Different measurements using the Josephson effect, Coulomb blockade, and scanning tunneling microscopes may provide additional information.

The Majorana fermions on the ends of quantum wires offer useful insights into the physics of non-Abelian systems. In the absence of the Majorana fermions, the ground state of a clean superconducting wire has an even number of electrons paired to Cooper pairs. Adding another electron is costly in energy, because this electron has no pairing partner. When the two Majorana fermions are localized at the ends of the wire, the odd electron can join at no cost of energy. The two degenerate ground states are then of different electron parities. When there are N wires, there are $2N$ zero modes and 2^N states, with each wire having either an even or odd number of electrons. This manner of counting explains the quantum dimension of $\sqrt{2}$.

Magic State Distillation and Surface Codes

Majorana fermions realize fusion and braiding rules analogous to those of "Ising anyons." Interchanging Majorana fermions at the ends of the same wire is equivalent to rotating the wire; this preserves the parity of the electron number while implementing a relative phase shift of $\pi/2$ between states of different parities. The braiding of two Majorana fermions of two different wires (Fig. 2) leads to a unitary transformation that takes the two wires from a state of well-defined parities to a state that is a superposition of even and odd parities, with equal probabilities. For example, the state $|\text{even1,even2}\rangle$ is transformed to the state $1/\sqrt{2}$ [$|\text{even1,even2}\rangle \pm i|\text{odd1,odd2}\rangle$], where the sign of the second term depends on the details of the interchange. Because only two types of interchanges are possible—intrawire and interwire—there is no topologically protected way to turn two wires that start, say, at even parities $|\text{even1,even2}\rangle$ into an arbitrary superposition of the

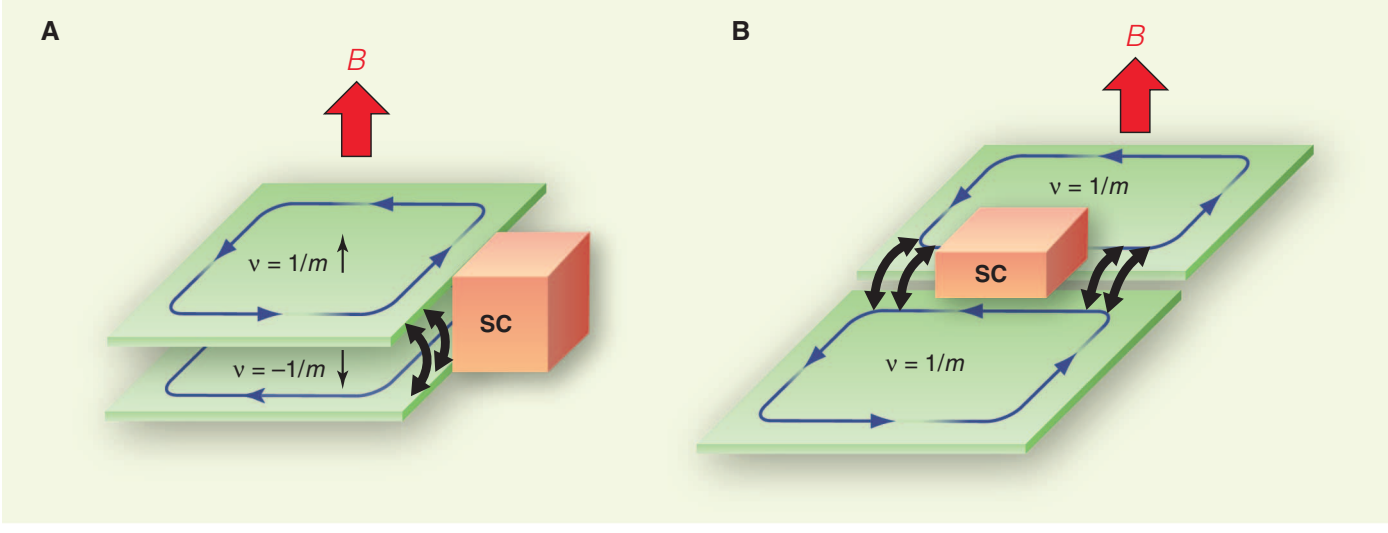

Fig. 4. Fractionalized Majorana zero modes at the interface between the superconductor and tunneling regions. (**A**) An electron-hole bilayer where the two layers are in a FQHE where the Hall conductivities are quantized at $\nu = \pm 1/m$ (in units of e^2/h), where m is an odd integer. The direction of the edge modes is indicated by the blue arrows. An s-wave superconductor (SC; orange) coupled to the edge of the two-layer system can gap the edge modes. In nonsuperconducting regions, spin-flipping electron tunneling between the top and bottom layer (black arrows) opens a gap on the edge. These can be enhanced by coupling the edge to a ferromagnet. Two layers of graphene may be a possible realization for such a system. (**B**) Single-layer realization, with a trench cut in a FQHE state with $\nu = 1/m$ exposing counterpropagating edge states. In spin-polarized quantum Hall states, spin-orbit interaction would couple these modes to a superconductor.

type $a|\text{even1,even2}\rangle \pm b|\text{odd1,odd2}\rangle$, with $|a| \neq |b|$. Topological quantum computation with Majorana fermions is therefore not universal (*4*–*6*). Using topologically protected braiding and measurement operations, Majorana fermions may carry out a set of gates known as the "Clifford gates." This set is generated by the single-qubit Hadamard gate, the single-qubit Pauli matrices, and the two-qubit CNOT gate (the latter requires a parity measurement of two qubits) (*13*). The gap to universal quantum computation may be bridged by adding a single-qubit gate that rotates the qubit by an angle $\pi/8$ (values other than $\pi/8$ are also possible).

Although topologically protected operations cannot implement the missing gate, they are able to approximate this gate with an arbitrarily small error, using a protocol called "magic state distillation" (*14*, *15*). The protocol consists of three key steps. First, nontopological operations create a large number of resource qubits in a "noisy" version of the state $|\psi_M\rangle = 1/\sqrt{2}\,[|0\rangle + \exp(i\pi/4)|1\rangle]$. [Note that there is no known way to accurately create the state $|\psi_M\rangle$ by using Clifford gates (i.e., topologically protected operations) alone.]

In the second step, one almost accurate qubit in the state $|\psi_M\rangle$ is distilled, using only topologically protected operations, from a large number of the noisy resource states. The possibility to do this endows $|\psi_M\rangle$ with the affectionate name "magic state." The distillation protocol is based on the concept of a "stabilizer" quantum error-correcting code (*33*). A quantum error-correcting code uses n physical qubits that span a space of 2^n states to represent one logical qubit. A unitary transformation takes a state of a single "logical" qubit and encodes it in this 2^n-dimensional space. As long as only a limited number of errors occur in the encoded state, they may be detected and corrected by measurements carried out on the n-qubit system, without disturbing the encoded quantum information.

In a stabilizer code, Pauli measurements and Clifford operations are sufficient for information encoding, decoding, and error correction. In the particular stabilizer code used for magic state distillation, Clifford operations can transform n qubits in the state $|\psi_M\rangle$ to an encoded logical state. Therefore, this code can be used to take n of the qubits that are noisy yet close enough to the state $|\psi_M\rangle$, encode them, detect the errors in their combined n-qubit state, keep only the error-free instances, and decode back to a single-qubit state. This entire step may be done in a topologically protected manner. Because the number of detectable errors is limited, this procedure cannot yield perfect magic states. However, the output is closer to the desired $|\psi_M\rangle$ than are the input resource states. This step can be applied repeatedly until the required level of accuracy is reached.

In the third and final step, the distilled magic states are used as ancillary qubits in order to apply the single-qubit rotation that is missing in the Clifford gates set. This is accomplished by measuring the joint parity of the logical qubit and the ancilla in the state $|\psi_M\rangle$. If the initial state of the logical qubit is $\alpha|0\rangle + \beta|1\rangle$, the measurement entangles the qubit and the ancilla either to the state $1/\sqrt{2}\,[\alpha|00\rangle + \beta \exp(i\pi/4)|11\rangle]$ or to $1/\sqrt{2}\,[\exp(i\pi/4)\alpha|01\rangle + \beta|10\rangle]$, depending on its outcome. A CNOT operation then disentangles the qubit from the ancilla, resulting in the required operation on the logical qubit. Magic state distillation complements the set of Clifford gates and opens the way to universal quantum computation based on Majorana fermions. The optimization of distillation protocols is currently under study (*34*).

In any physical realization of topological quantum computing, we must still expect an inevitable amount of errors. A promising approach for dealing with these errors is to incorporate topological qubits into a particularly fault-tolerant class of stabilizer codes, known as "surface codes." These codes consist of a 2D or 3D array of qubits (*3*, *35*). In surface codes, the states used to encode the logical qubit are the ground states of a Hamiltonian that describes couplings between different physical qubits in the array. This Hamiltonian gives rise to Abelian anyons. Two Abelian anyons have only one fusion outcome and therefore do not have the full advantages of their non-Abelian counterparts. Nonetheless, the surface codes do offer an enhanced robustness to decoherence and noise. The logical quantum information is encoded by the presence or absence of Abelian anyons on holes cut out in the array. An error occurring in a surface code amounts to creating an excited anyon–anti-anyon pair, which can be located and corrected by performing Pauli measurements and Clifford operations on the code's qubits. The error tolerance of surface codes can be several orders of magnitude better than most other known types of quantum error-correcting codes, but it comes at the price of the large number of physical qubits needed to encode a single logical qubit.

The ideas outlined above have inspired several proposals for hybrid structures of topological and nontopological components. These structures either combine nonprotected superconducting qubits or charge qubits with protected Majorana qubits, or combine protected quantum Hall interferometric gates with nonprotected parts (*36*–*41*). The role of the nontopological parts is limited to the operations that cannot be carried out in a protected manner, requiring effective and fast control of the coupling of the nontopological and topological parts.

Non-Abelian Anyons in Quantum Hall Systems

Non-Abelian anyons with properties richer than those of Majorana fermions are known in several systems. Below, we survey non-Abelian anyons on the edges of Abelian quantum Hall systems (*42*–*47*) and non-Abelian quantum Hall states (*1*, *2*, *10*, *16*, *48*).

The 2D gapped bulk of the quantum Hall effect is accompanied by 1D gapless edge modes. These modes occur at the interface of a quantum Hall state with the vacuum, between quantum Hall states of different filling factors, or even between quantum Hall states of the same filling factor and different spin polarization. We focus here on cases where gapless modes flow in both directions; these modes may be gapped by a perturbation that induces backscattering between them. One such case (Fig. 4A) is bilayer electron-hole system, in which the electrons and the holes are subjected to the same magnetic field and have the same densities. Because of their opposite charges, the two layers carry counterpropagating edge modes in physical proximity. When the values of the quantized Hall conductivities at the two layers (in units of e^2/h) are $\nu = \pm 1/m$, there is one mode flowing in each of the layers; in more complicated cases, there may be several such modes. Counterpropagating edge modes can also be realized in single-layer systems (Fig. 4B).

For $\nu = \pm 1/m$, the two counterpropagating edge modes may be gapped when they are both coupled either to a superconductor or to a ferromagnet (Fig. 4). In the two-layer case, the superconductor exchanges pairs of electrons with the two layers, one electron with each layer, whereas the ferromagnet scatters an electron from one layer to the other. In more complicated cases, there may be other ways to gap the edges, even with no superconductivity present. If different regions of the edge are gapped by different mechanisms, zero modes may appear at the interfaces between these regions. For $m = 1$, these are Majorana fermion zero modes, with quantum dimension $\sqrt{2}$. For the fractional case $m > 1$, the emerging anyons have a larger quantum dimension of $\sqrt{2m}$. In these cases, the regions on the edge that are coupled to superconductors form "superconducting quantum wires" and are otherwise surrounded by an insulating bulk. Their charge is then quantized modulo the charge of a Cooper pair. The quantization unit is the elementary charge of the surrounding medium, which is $1/m$ of the electron charge, resulting in $2m$ possible charge values.

The non-Abelian anyons that are realized on the gapped edges of Abelian quantum Hall systems may be braided using operations of the form outlined in Fig. 2. The unitary transformations that are realized by such braiding are richer than those realized by Majorana fermions. Unfortunately, these systems do not allow for universal quantum computation; however, they are robust to electronic noise and allow all Clifford operations to be performed using braiding. The precise computational potential of the non-Abelian anyons on edges of Abelian quantum Hall states has not yet been fully explored (*47*).

With respect to universal quantum computation, the most powerful anyons may be realized in the fractional quantum Hall effect (FQHE), in particular for states in the Landau level range of $2 < \nu < 4$. The non-Abelian anyons

in this system are fractionally charged quasiparticles. Despite the differences between these and the systems described above in the context of Majorana fermions, there are similarities in the path that may lead to the formation of non-Abelian anyons. In both systems, the interaction between electrons leads to states that may be viewed as a Bose-Einstein condensate. For superconductors, the condensed particles are Cooper pairs composed of two electrons each. For non-Abelian FQHE states, the condensed bosons are clusters of k electrons, with $k + 2$ magnetic flux quanta attached. The attached flux transmutes the electrons into Abelian anyons, and k of these anyons form the boson that condenses. The resulting state is a candidate state for Landau level fillings of $\nu = L + [2/(k + 2)]$ and $\nu = L + [k/(k + 2)]$, where L is the number of filled inert Landau levels. On the basis of numerical analysis, the most likely range of fillings where these states may be energetically favorable to other states has $L = 2$. These states are usually referred to as the Moore-Read state (for $k = 2$) (*1*) and the Read-Rezayi states (for $k \geq 3$) (*48*).

Similar to Majorana fermions, Moore-Read non-Abelian quasiparticles (*1*) have the quantum dimension of $\sqrt{2}$. For the Read-Rezayi states, the fractional statistics of the k anyons makes the counting of the ground states quite complicated. Briefly, the quantum dimension of the resulting non-Abelian anyons is $2\cos[\pi/(k + 2)]$, which is not a square root of an integer. The transformations implemented when the non-Abelian anyons of $k \neq 2$ or 4 are braided are rich enough to enable a universal set of quantum gates.

Numerical and experimental evidence (Fig. 3E) supports the identification of the $\nu = 5/2$ state as a Moore-Read state (*49*–*52*). Experimental investigation of states with $k \geq 3$ has so far been hindered by their fragility, reflected in a small energy gap and strong sensitivity to disorder.

The non-Abelian anyons realized by fractionally charged quasiparticles in FQHE states are full-fledged quantum dynamical degrees of freedom, in contrast to those realized by zero modes confined to vortices or interfaces between phases. This difference is reflected in the way of measuring the fusion outcome of two anyons. For a pair of zero modes at two ends of a superconducting wire, the outcome can be measured by interfering a vortex around the superconductor and then measuring the phase shift induced by the Aharonov-Casher effect (*53*). In contrast, for the FQHE anyons, qubit measurements can be carried out by interfering the anyons themselves (*54*–*56*). We note that the unitary transformations required for topological quantum computing can be simulated using only measurements of fusion outcomes (instead of performing braiding operations) (*57*).

Outlook

The field of topological quantum computation is in its infancy. On the experimental side, there has been substantial recent progress in the study of systems that host Majorana fermions. So far, this study has mostly attempted to demonstrate the existence of these Majorana fermions. In the near future, one may expect further experiments aimed at nailing down the identification of these systems as non-Abelian, together with the development of methods to control, manipulate, and braid the anyons. Concurrently, one may expect experimental attempts to form hybrids of topological and nontopological qubits. These experiments will surely benefit from detailed theoretical modeling of the experimental systems. Future theoretical studies will hopefully propose novel non-Abelian systems that could be realized experimentally. These studies will benefit from an ongoing effort to classify non-Abelian states and explore the underlying mathematical structures. On the quantum computer science front, much remains to be understood regarding the computational power of various types of non-Abelian systems. Future studies may refine the distinction between universal and nonuniversal quantum computation, and distinguish between more and less powerful schemes for nonuniversal quantum computation.

References and Notes

1. G. Moore, N. Read, *Nucl. Phys. B* **360**, 362 (1991).
2. C. Nayak, S. H. Simon, A. Stern, M. Freedman, S. Das Sarma, *Rev. Mod. Phys.* **80**, 1083 (2008), and references therein.
3. A. Yu. Kitaev, *Ann. Phys.* **303**, 2 (2003).
4. M. H. Freedman, M. Larsen, Z. Wang, *Comm. Math. Phys.* **227**, 605 (2002).
5. M. Freedman, C. Nayak, K. Walker, *Phys. Rev. B* **73**, 245307 (2006).
6. J. Preskill, Lecture Notes on Quantum Computation (www.theory.caltech.edu/~preskill/ph219/topological.pdf).
7. A. Stern, *Nature* **464**, 187 (2010).
8. J. Alicea, *Rep. Prog. Phys.* **75**, 076501 (2012).
9. A. Kitaev, *Ann. Phys.* **321**, 2 (2006).
10. C. Nayak, F. Wilczek, *Nucl. Phys. B* **479**, 529 (1996).
11. The degeneracy of the ground state is never perfect. The energy splitting between the different ground states is exponentially small in the ratio of the anyons' separation and a (system-dependent) microscopic length scale. It can thus be made arbitrarily small by increasing this separation.
12. A. Yu. Kitaev, *Russ. Math. Surv.* **52**, 1191 (1997).
13. M. A. Nielsen, I. L. Chuang, *Quantum Computation and Quantum Information* (Cambridge Univ. Press, Cambridge, 2000).
14. S. Bravyi, A. Yu. Kitaev, *Phys. Rev. A* **71**, 022316 (2005).
15. S. Bravyi, *Phys. Rev. A* **73**, 042313 (2006).
16. N. Read, D. Green, *Phys. Rev. B* **61**, 10267 (2000).
17. A. Yu. Kitaev, *Phys. Uspekhi* **44** (suppl. 10), 131 (2001).
18. D. A. Ivanov, *Phys. Rev. Lett.* **86**, 268 (2001).
19. A. Stern, F. von Oppen, E. Mariani, *Phys. Rev. B* **70**, 205338 (2004).
20. J. Alicea, Y. Oreg, G. Refael, F. von Oppen, M. P. A. Fisher, *Nat. Phys.* **7**, 412 (2011).
21. B. I. Halperin *et al.*, *Phys. Rev. B* **85**, 144501 (2012).
22. J. D. Sau, D. J. Clarke, S. Tewari, *Phys. Rev. B* **84**, 094505 (2011).
23. L. Fu, C. L. Kane, *Phys. Rev. Lett.* **100**, 096407 (2008).
24. L. Fu, C. L. Kane, *Phys. Rev. B* **79**, 161408 (2009).
25. J. D. Sau, R. M. Lutchyn, S. Tewari, S. Das Sarma, *Phys. Rev. Lett.* **104**, 040502 (2010).
26. R. M. Lutchyn, J. D. Sau, S. Das Sarma, *Phys. Rev. Lett.* **105**, 077001 (2010).
27. Y. Oreg, G. Refael, F. von Oppen, *Phys. Rev. Lett.* **105**, 177002 (2010).
28. V. Mourik *et al.*, *Science* **336**, 1003 (2012).
29. A. Das *et al.*, *Nat. Phys.* **8**, 887 (2012).
30. A. D. K. Finck, D. J. Van Harlingen, P. K. Mohseni, X. Li, K. Jung, http://arXiv.org/abs/1212.1101 (2012).
31. L. P. Rokhinson, X. Liu, J. K. Furdyna, *Nat. Phys.* **8**, 795 (2012).
32. M. T. Deng *et al.*, *Nano Lett.* **12**, 6414 (2012).
33. D. Gottesman, http://arxiv.org/abs/quant-ph/9705052 (1997).
34. G. Duclos-Cianci, K. M. Svore, http://arXiv.org/abs/1210.1980 (2012).
35. E. Dennis, A. Yu. Kitaev, A. Landahl, J. Preskill, *J. Math. Phys.* **43**, 4452 (2002).
36. F. Hassler, A. R. Akhmerov, C.-Y. Hou, C. W. J. Beenakker, *N. J. Phys.* **12**, 125002 (2010).
37. P. Bonderson, D. J. Clarke, C. Nayak, K. Shtengel, *Phys. Rev. Lett.* **104**, 180505 (2010).
38. E. Grosfeld, A. Stern, *Proc. Natl. Acad. Sci. U.S.A.* **108**, 11810 (2011).
39. L. Jiang, C. L. Kane, J. Preskill, *Phys. Rev. Lett.* **106**, 130504 (2011).
40. P. Bonderson, R. M. Lutchyn, *Phys. Rev. Lett.* **106**, 130505 (2011).
41. F. Hassler, A. R. Akhmerov, C. W. J. Beenakker, *N. J. Phys.* **13**, 095004 (2011).
42. N. H. Lindner, E. Berg, G. Refael, A. Stern, *Phys. Rev. X* **2**, 041002 (2012).
43. D. J. Clarke, J. Alicea, K. Shtengel, *Nat. Commun.* **4**, 1348 (2013).
44. M. Cheng, *Phys. Rev. B* **86**, 195126 (2012).
45. A. Vaezi, *Phys. Rev. B* **87**, 035132 (2013).
46. M. Barkeshli, C.-M. Jian, X.-L. Qi, *Phys. Rev. B* **87**, 045130 (2013).
47. M. B. Hastings, C. Nayak, Z. Wang, http://arXiv.org/abs/1210.5477 (2012).
48. N. Read, E. Rezayi, *Phys. Rev. B* **54**, 16864 (1996).
49. M. Storni, R. H. Morf, S. Das Sarma, *Phys. Rev. Lett.* **104**, 076803 (2010).
50. R. L. Willett, L. N. Pfeiffer, K. W. West, *Phys. Rev. B* **82**, 205301 (2010).
51. A. Bid *et al.*, *Nature* **466**, 585 (2010).
52. S. An *et al.*, http://arXiv.org/abs/1112.3400 (2011).
53. Y. Aharonov, A. Casher, *Phys. Rev. Lett.* **53**, 319 (1984).
54. S. Das Sarma, M. Freedman, C. Nayak, *Phys. Rev. Lett.* **94**, 166802 (2005).
55. A. Stern, B. I. Halperin, *Phys. Rev. Lett.* **96**, 016802 (2006).
56. P. Bonderson, A. Kitaev, K. Shtengel, *Phys. Rev. Lett.* **96**, 016803 (2006).
57. P. Bonderson, M. Freedman, C. Nayak, *Ann. Phys.* **324**, 787 (2009).
58. R. L. Willett, C. Nayak, K. Shtengel, L. N. Pfeiffer, K. W. West, http://arXiv.org/abs/1301.2639 (2013).

Acknowledgments: We thank C. Nayak and J. Preskill for helpful discussions, and the Kavli Institute for Theoretical Physics for their hospitality. Supported by the U.S.-Israel Binational Science Foundation, the Minerva foundation, and Microsoft Station Q (A.S.); Defense Advanced Research Projects Agency award N66001-12-1-4034 and the Institute for Quantum Information and Matter, an NSF Physics Frontiers Center, with support of the Gordon and Betty Moore Foundation (N.H.L.); and NSF grant PHY11-25915.

10.1126/science.1231473